nature chemical biology

ARTICLE

PUBLISHED ONLINE: 2 MAY 2010 | DOI: 10.1038/NCHEMBIO.363

Small molecules discovered in a pathway screen target the Rho pathway in cytokinesis

Adam B Castoreno[1], Yegor Smurnyy[1], Angelica D Torres[1], Martha S Vokes[2], Thouis R Jones[2], Anne E Carpenter[2] & Ulrike S Eggert[1]*

We report the discovery of small molecules that target the Rho pathway, which is a central regulator of cytokinesis—the final step in cell division. We have developed a way of targeting a small molecule screen toward a specific pathway, which should be widely applicable to the investigation of any signaling pathway. In a chemical genetic variant of a classical modifier screen, we used RNA interference (RNAi) to sensitize cells and identified small molecules that suppressed or enhanced the RNAi phenotype. We discovered promising candidate molecules, which we named Rhodblock 1–8, and we identified the target of Rhodblock 6 as Rho kinase. Several Rhodblocks inhibited one function of the Rho pathway in cells: the correct localization of phosphorylated myosin light chain during cytokinesis. Rhodblocks differentially perturb Rho pathway proteins in cells and can be used to dissect the mechanism of the Rho pathway during cytokinesis.

Rho GTPases are key regulators of cell division and control other processes that involve the cytoskeleton, such as cell migration, contraction and adhesion[1]. With Rho GTPases at the center of complicated signaling cascades that are only partially understood, different branches of these pathways cooperate to coordinate these processes. Small GTPases regulate their downstream effectors by switching between two states, active (GTP-bound) and inactive (GDP-bound)[1]. This cycling is controlled by regulatory proteins such as guanine nucleotide exchange factors (GEFs) and GTPase-activating proteins (GAPs). Improper regulation of the Rho pathway has been implicated in cardiovascular diseases and cancer[2,3]. For example, RhoA is highly overexpressed in breast tumors and malignancy is correlated with high RhoA expression[4,5]. There is increasing evidence that altered Rho signaling contributes to cancer onset, invasion and metastasis, but little is known about the underlying mechanisms of this process[6,7]. In this study, we focus on the role of the Rho pathway in cytokinesis, the final step of cell division, in which cells physically separate[8]. As a key regulator, the Rho pathway participates in all steps of cytokinesis, from the initial specification of the location of the cleavage furrow, to constriction and final abscission. Small molecules that target the Rho pathway would be very useful, both as biological probes and as therapeutic leads[9,10].

Until now, there have been limited options for identifying small molecules that affect pathways. Pure protein screens target single proteins, whereas phenotypic screens target entire processes, irrespective of a specific pathway. Despite serious efforts, especially with the oncogenic GTPase Ras, small molecules that target the GTP-binding pocket in small GTPases have been elusive because GTP affinity in GTPases is much higher than ATP affinity in kinases[11]. This is why we decided to develop a strategy to target the GTPase signaling pathway rather than the GTPase's enzymatic activity. Rho associates with many regulatory and downstream effector proteins, which are potential small molecule targets. It is difficult to target these proteins using conventional biochemical assays because inhibition of their enzyme activity is often not readily detectable. Here, we report the development of a phenotypic screening approach that allows us to target a pathway independent of specific enzyme activities. We identify pathway-specific small molecules and show that they perturb the Rho pathway in cells.

RESULTS

Screen concept and design

Our goal was the identification of small molecules that specifically target the Rho pathway. Inspired by classical genetic experiments, we designed a phenotypic screening strategy analogous to a genetic modifier screen, but perturbed cells using small molecules and RNA interference (RNAi), instead of genetic mutations. By using RNAi to impair signaling through the Rho pathway, we decreased the amount of compound needed to detect a phenotype. To ensure specificity, we prioritized compounds that exhibited stronger defects in RNAi-sensitized cells than in wild-type cells.

We used the success or failure of cytokinesis as a measure of Rho activity. Failed cytokinesis leads to the formation of binucleated cells, which was the readout in the screen. We chose to deplete Rho itself because it is tractable, ideally positioned within the signaling cascade and biologically and clinically relevant. We modestly impaired cytokinesis using partial RNAi depletion of Rho, added small molecules, and identified compounds that suppressed or aggravated RNAi-induced cytokinesis defects (**Fig. 1a**). We expected to find enhancers and suppressors because the pathway is both positively and negatively regulated.

A key feature of our strategy is to achieve an intermediate RNAi phenotype. During RNAi in *Drosophila* cells, which we used in this screen, double-stranded (ds)RNA corresponding in sequence to mRNA encoding the target protein is added to cells. The mRNA is destroyed, and no new protein can be synthesized, resulting in the depletion of the target protein over time. We used the gradual decrease in Rho protein during RNAi treatment to obtain our intermediate phenotype. We optimized the assay to reproducibly yield intermediate depletion of Rho by varying the sequence and dose of the dsRNA and the length of the RNAi experiment (**Supplementary Fig. 1**).

[1]Dana-Farber Cancer Institute and Department of Biological Chemistry and Molecular Pharmacology, Harvard Medical School, Boston, Massachusetts, USA. [2]The Broad Institute of Harvard and MIT, Cambridge, Massachusetts, USA. *e-mail: ulrike_eggert@dfci.harvard.edu

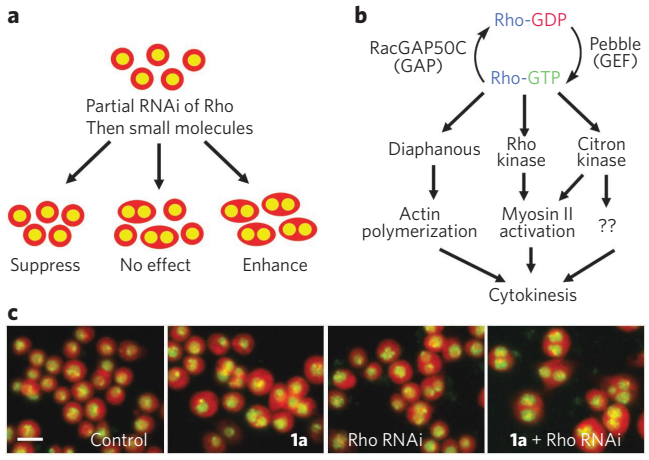

Figure 1 | Screening strategy to identify small molecules that target the Rho pathway. (a) A small molecule/RNAi modifier screen. Cells are drawn in red, nuclei in yellow. (**b**) Simplified diagram of Rho signaling during cytokinesis. (**c**) Example of synergy between Rho RNAi and a hit compound (Rhodblock **1a**). Note how the percentage of binucleate cells is relatively low in cells that are treated with RNAi or compound, but increases in cells treated with both RNAi and compound (*Drosophila* Kc167 cells are shown in red, nuclei in yellow). Scale bar, 10 μm.

Synergy between Rho pathway proteins

We first confirmed that the concept of the screen was feasible; that is, that we could observe synergy, measured as a substantial increase in binucleate cells that is larger than the effect of two independent treatments, if we blocked different branches of the Rho pathway at the same time. We performed double RNAi experiments where two different pathway proteins (see **Fig. 1b** for examples) were depleted simultaneously and observed synergy between these protein pairs (**Supplementary Fig. 2**). Conversely, we did not observe synergy between Rho RNAi and RNAi of proteins or small molecule inhibitors that target cytokinesis, but not the Rho pathway (**Supplementary Methods**). It is important to include such Rho-independent controls because the screen could potentially result in other outcomes such as the identification of small molecules that modulate the process of RNAi itself.

We also confirmed that we could observe synergy between Rho RNAi and pathway-specific small molecule treatment. When we tested GSK269962A[12], a Rho kinase inhibitor, we observed strong synergy with Rho RNAi. Our screening concept predicts that a compound that is specific for the Rho pathway should inhibit cytokinesis in non-RNAi treated cells at higher concentrations than in cells sensitized by RNAi treatment, which is what we observed with GSK269962A (**Supplementary Fig. 3**).

Automated image analysis

Although the human eye can readily detect changes in the ratio of mononucleate to binucleate cells (**Fig. 1c**), an important challenge in the development of our screening protocol was to automate the image analysis, both to allow high throughput and to quantify our screening output. We used the CellProfiler software package[13] and its machine learning capability[14] to differentiate between cells with one nucleus and those with two nuclei using machine learning guided by visual inspection (**Supplementary Methods** and **Supplementary Fig. 4**).

Nine small molecule enhancers of Rho RNAi

We screened ~38,000 compounds from commercial sources and natural product extracts. During the screen, we arrayed RNAi-treated (or wild-type) *Drosophila* Kc_{167} cells into 384-well plates, treated them with small molecules (nominal concentration ~25 μM), fixed the cells and stained cells and DNA with fluorescent markers. We collected images by automated fluorescence microscopy and performed automated image analysis to identify wells containing active small molecules (**Supplementary Table 1**). To calibrate our screen, we first screened a collection of compounds with known biological activities. In addition to enhancers, we found several compounds that suppressed the RNAi phenotype, that is, they inhibited the formation of binucleate cells (**Supplementary Table 2**). Most of these compounds were cell cycle inhibitors that arrest cells before they get to the division stage. To ensure that the suppressors we indentified in the full screen target the Rho pathway rather than a different step earlier in the cell cycle, a careful cell cycle analysis is needed for this class of compounds. We therefore initially focused on enhancers and selected the nine most active compounds, which we named Rhodblock **1a**,**b**–**8**, for further evaluation. Each compound caused a substantial increase in the proportion of binucleate cells in a partial Rho RNAi background (**Fig. 1c**).

We purchased the nine Rhodblocks, confirmed their identity by analytical chemistry and tested them at different concentrations to determine the minimal concentration at which we could observe robust synergy with Rho RNAi (**Table 1**). To rule out possible effects on RNAi rather than synergy with the Rho pathway, we tested the active compounds in cells treated with a protein inhibitor of Rho, C3 transferase (CT04)[15]. All compounds synergized with CT04 as well as with Rho RNAi. As predicted by our screening concept and the GSK269962A experiment discussed above, we would expect the Rhodblocks to be active in the absence of Rho RNAi at higher concentrations. Rhodblock **1a**, our most active compound, was active at 100 μM and synergized with Rho RNAi at 10 μM. Our collection of active compounds included the small molecule Rhodblock **1b**, which was structurally related to Rhodblock **1a**, allowing a rudimentary structure–activity analysis. To evaluate the importance of the substituents on Rhodblock **1**, we obtained compound **1c**, which varies from **1a** only in the furan substituent (**Supplementary Fig. 5**). The activity of **1c** was similar to that of the less active **1b**, suggesting that the furan is an important determinant of activity.

Quantification of synergy

To gain a more quantitative understanding of the strength of the synergistic interactions between our compounds and Rho RNAi, we calculated a 'synergy ratio' (**Table 1**). We define the synergy ratio as the ratio of the observed phenotype over the expected phenotype. If the effects of small molecule treatment and partial Rho RNAi are independent of each other, they can be represented in a multiplicative model; the resulting phenotype would constitute

Table 1 | Synergy ratios for Rhodblocks 1–8 in cells sensitized by partial RNAi of Rho pathway proteins

Rhodblock	Rho	Pbl	RacGAP	Dia	CK	Rok
1a (10 μM)	14.7	2.3	2.1	1.3	0.7	0.9
1b (30 μM)	8.1	0.9	1.1	0.8	0.2	0.7
2 (30 μM)	4.0	4.2	1.1	2.7	0.7	1.7
3 (100 μM)	9.0	1.9	0.4	1.4	0.8	0.7
4 (30 μM)	2.9	2.1	1.7	2.3	0.8	1.5
5 (100 μM)	5.9	1.8	0.7	1.1	0.7	0.8
6 (100 μM)	3.5	2.6	0.6	1.3	0.8	1.9
7 (30 μM)	3.0	1.4	1.5	1.2	0.8	0.5
8 (30 μM)	4.0	2.0	1.1	0.8	0.7	1.2

Strong interactions (synergy ratio >4) are highlighted in red, moderate interactions (2–4) in orange and weaker interactions (1.3–2) in yellow. Insignificant changes (0.7–1.2) are pale yellow and antagonistic interactions pale green. See Methods and **Supplementary Information** for data and details on the statistical analysis. Rho, RhoA; Pbl, pebble; RacGAP, RacGAP50C; Dia, Diaphanous; CK, Citron kinase; Rok, Rho kinase.

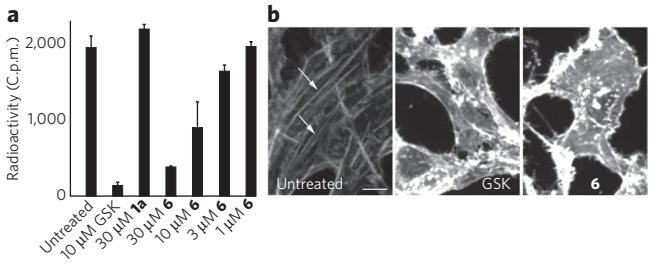

Figure 2 | Rhodblock 6 inhibits Rho kinase. (**a**) *Drosophila* Rho kinase assay data for Rhodblock **6**. A dose-response chart is shown as well as control data for the Rho kinase inhibitor GSK269962A and Rhodblock **1a**. For full panel, see **Supplementary Figure 6**. Error bars indicate s.d. (n = 2). (**b**) Rhodblock **6** (100 μM) and GSK269962A (10 μM) cause disappearance of actin stress fibers in HeLa cells (white arrows in control image). HeLa cells were treated for 20 h and fixed. Actin was visualized using phalloidin staining. Scale bar, 10 μm.

the 'expected phenotype'. All compounds selected for this study have a synergy ratio of ~3 or higher for Rho RNAi (**Table 1**), meaning that the observed synergistic phenotype shows at least a threefold increase relative to the background.

Rhodblocks synergize with other Rho pathway proteins

After establishing synergy with Rho RNAi, we explored the Rhodblocks' interactions with other Rho pathway proteins. As our screen targets a pathway rather than a single protein, we expected to obtain compounds that target different proteins within the Rho pathway. Because each protein within the pathway has different functions and interaction partners, compounds that target different proteins should show different levels of synergy with other pathway proteins. We therefore analyzed the effects of the Rhodblocks on cells in which other Rho pathway proteins had been partially depleted by RNAi (**Table 1**). We chose the regulatory GAP (called RacGAP50C in *Drosophila*[16], MgcRacGAP in mammals[17] and cyk-4 in *C. elegans*[18]) and GEF (called pebble in *Drosophila*[19], Ect2 in mammals) proteins as well as the effector proteins Diaphanous[20], Rho kinase and Citron kinase (**Fig. 1b**). We quantified synergistic interactions for each small molecule/RNAi pair and showed that each compound has a unique synergy pattern (**Table 1** and **Supplementary Tables 3** and **4**).

We performed the entire panel in parallel to reduce error due to experimental variations and used conditions optimized for Rho RNAi, which could explain why the highest synergy ratios were observed in cells sensitized by Rho RNAi. For example, we observed relatively low synergy ratios with Rho kinase RNAi. Rho kinase is a stable protein and it has been reported that extended RNAi treatments are needed to observe a robust phenotype[21]. When we sensitized cells by longer treatment with Rho kinase RNAi, we observed an increase in synergy at lower concentrations of Rhodblock **6** (see below). Some compounds showed both synergy and antagonism (that is, some suppressed the RNAi phenotype rather than enhancing it), especially in RacGAP-sensitized cells. RacGAP is thought to have opposing roles as a Rho deactivator and as a scaffold required for correct Rho localization and activation[22], which could explain positive and negative interactions with our small molecules. We conclude from these experiments that our compounds are likely to have diverse targets within the Rho pathway.

Rhodblock 6 inhibits Rho kinase

To further support our initial strong, but circumstantial, evidence that we have discovered compounds that target the Rho pathway, we wanted to measure directly the inhibition of Rho pathway activity, both *in vitro* and in cells. There are no specific biochemical assays for many proteins in the pathway. However, Rho kinase (Rok in *Drosophila*) can be readily assayed in a kinase assay. We purified FLAG-tagged Rok and tested our compounds at the concentrations at which we observed synergy in cells (**Table 1**, **Supplementary Fig. 6**). Rhodblock **6** inhibited Rok activity robustly and in a dose-dependent manner (**Fig. 2**). It also inhibited its human ortholog, ROCK I (**Supplementary Fig. 7**) and, like other ROCK inhibitors, it caused the disruption of stress fibers in human HeLa cells (**Fig. 2**). The formation of stress fibers in human cells is one of the functions of the Rho pathway that is mediated by ROCK[23]. Rok's functions during cytokinesis include the phosphorylation of myosin regulatory light chain (see below) and the inhibition of myosin phosphatase (*Drosophila* Mbs). Mbs and Rok have antagonistic functions and Mbs RNAi can partially rescue Rok RNAi phenotypes[21]. We observed a considerable reduction in binucleate cells when Mbs was depleted in Rhodblock 6–treated cells (**Supplementary Table 5**). These data suggest that Rok is a meaningful cellular target of Rhodblock **6** and provide further evidence that our screen can identify compounds that target the Rho pathway.

Rhodblocks inhibit a cellular function of the Rho pathway

We next investigated whether our Rhodblock compounds affected a specific function of the Rho pathway in cells, which would be the most conclusive validation of our approach and is a key feature in our goal to use these compounds as small molecule probes. Several proteins in the pathway, including Rok, cooperate to localize myosin II at the cleavage furrow and activate it by phosphorylating Ser21 on myosin regulatory light chain (MRLC) in *Drosophila* cells[24]. By using a phospho-specific antibody, we can evaluate whether this branch of the Rho pathway has been perturbed. Treatment of cells with eight (Rhodblocks **1**–**6** and **8**) of the nine Rhodblocks at the lowest synergistic concentration caused a variably penetrant decrease in phosphorylated MRLC and its mislocalization from the cleavage furrow (**Fig. 3**). We expected to observe this phenotype for Rhodblock **6** because it inhibits Rok, a protein involved in myosin phosphorylation. The other Rhodblocks, however, do not inhibit Rok *in vitro*, suggesting that they target different proteins in the pathway. As myosin phosphorylation is just one of the cellular functions of the Rho pathway, we expect the compound that did not inhibit myosin phosphorylation to target a different branch of the Rho pathway.

Rhodblocks perturb key cytokinesis proteins

After establishing that most of our compounds inhibit a function of the Rho pathway, our next goal was to study the role of the pathway during cytokinesis. We did this initially by evaluating the localization of Rho pathway proteins in the presence of small molecules. We focused on Rhodblocks **1a**, **3** and **6** because they show potent synergy with Rho RNAi and are the most penetrant inhibitors of MRLC phosphorylation (that is, we know that they target the Rho pathway). To minimize possible off-target effects, we performed all detailed cellular studies using the Rhodblocks at their minimal synergistic concentrations and amplified the effects of our small molecules with an overnight Rho RNAi treatment before small molecule addition. We saw no significant reduction in the number of cytokinetic cells showing decreased Rho staining at the cleavage furrow after overnight treatment (**Supplementary Fig. 8**). Unlike in the screen, where we treated sensitized cells with small molecules for 24 h to allow most cells to complete a cell cycle and to enter (and fail) cytokinesis, we used a shorter (4 h) treatment in the detailed studies. Although fewer cells will be in the process of failing cytokinesis, failure will be acute, allowing us to analyze the localization of cytokinesis proteins at the cleavage site before cells adapt to the new conditions. The ability to use acute treatments is an important advantage of small molecules over genetic approaches such as RNAi.

Efforts to dissect signaling cascades in the Rho pathway have primarily focused on evaluating the localization patterns of pathway

proteins. Many Rho pathway proteins that are involved in cytokinesis are co-dependent for localization, and the requirement of one protein for correct localization of a second suggests that the first protein is upstream of the second in the signaling cascade. Correct localization does not mean that a particular protein is active, but in the absence of assays for protein activity for many Rho pathway proteins, it gives some indication as to their function. We therefore analyzed the effects of our compounds on proteins that localize to the ingressing cleavage furrow such as actin, phospho-MRLC (see above), Anillin, a septin (*Drosophila* Peanut) and Rho itself. We also analyzed microtubule structures as well as RacGAP and the kinesin-6 Pavarotti (called MKLP1 in mammals), which form the microtubule-bound Centralspindlin complex[25]. For a discussion of these proteins in the context of their role during cytokinesis, see Discussion. The three Rhodblocks we chose for further analysis showed different localization patterns for different proteins, further supporting our hypothesis that they target different proteins in the pathway (**Fig. 3**). None of the compounds disrupted Centralspindlin localization, and only Rhodblock **1a** had an effect on microtubule structures. Instead of forming a single midzone microtubule bundle, midzone microtubules in cells treated with Rhodblock **1a** often bundled into two or more structures (**Figs. 3** and **4**). Rhodblock **6**, the Rok inhibitor, inhibited phospho-MRLC localization but did not have an effect on other proteins. Rhodblock **3** inhibited phospho-MRLC localization as well as furrow localization of the septin Peanut and increased Peanut's localization on microtubules but did not affect any of the other proteins we tested. Relocalization of Peanut to midzone microtubules has been reported to result from treatment with Anillin RNAi[26]. By contrast, Rhodblock **1a** inhibited furrow localization of the cortical proteins we tested (Actin, Anillin, Peanut), with Peanut strongly associating with microtubules. Rho was also mislocalized in about 50% of cells (**Supplementary Fig. 9**).

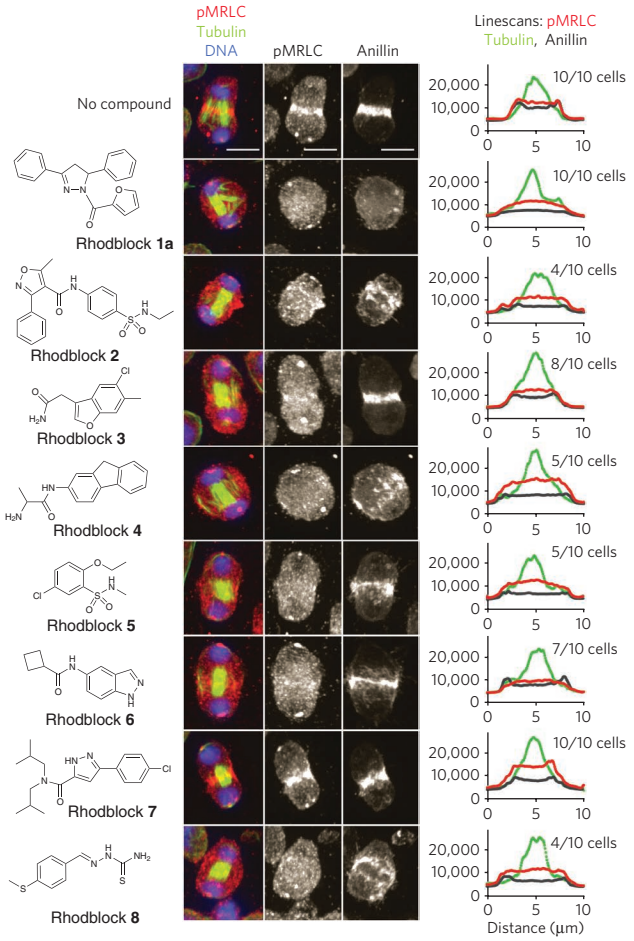

Figure 3 | Several Rhodblocks prevent the accumulation of phospho-myosin regulatory light chain and/or Anillin at the cleavage furrow. The chemical structures of Rhodblocks **1**–**8** are shown on the left. Immunofluorescence images of representative phenotypes for each Rhodblock are shown in the middle. Phospho-MRLC (red), tubulin (green) and DNA (blue) have been visualized in *Drosophila* Kc_{167} cells. For greater clarity, the middle panel shows gray-scale images of phospho-MRLC staining only. The right panel shows gray-scale images of Anillin staining in the same cell. The images were taken under identical conditions and were processed identically (see **Supplementary Methods**). Scale bar, 5 μm. We analyzed images of ten cells for each condition (4 h treatment with compound at the minimally synergistic concentration after overnight Rho RNAi sensitization). For each cell we analyzed, we placed a line across the cleavage furrow and quantified the fluorescence intensities for phospho-MRLC, Anillin and tubulin staining (see **Supplementary Methods**). We then averaged the linescans for cells exhibiting the phospho-MRLC phenotype shown in this figure (on the right). The number of cells represented by the image is indicated in parentheses above the linescans for each compound. In the linescans, the *x* axis represents fluorescence intensity in arbitrary units (AU). Bumps in fluorescence intensities at the edge of the cell are characteristic of an intact furrow (for example, control cell), uniform fluorescence intensities across the entire cell are characteristic of a missing furrow (for example, Rhodblock **1a**). In Rhodblock **6**-treated cells, Anillin forms a furrow whereas phospho-MRLC does not.

Focusing in more detail on Rhodblocks **1a**, **3** and **6**, we have shown that these compounds have different effects on cytokinesis proteins. We conclude from these data that our compounds are useful probes to dissect the role of the Rho pathway in cytokinesis.

DISCUSSION

Combining different types of perturbations, for example genetic and small molecule treatments, can expand our understanding of complex biological processes[27]. Here, we report a strategy for discovering small molecules that target signaling pathways, by combining small molecule treatments with RNAi. Cells are sensitized to small molecules by lowering the levels of Rho, a key protein in the Rho signaling pathway. Reducing the amount of target protein in a cell to identify specific small molecule ligands has been used successfully in the discovery of antibiotics[28]. Despite the appeal of this strategy, it has been difficult to adapt it to higher organisms because

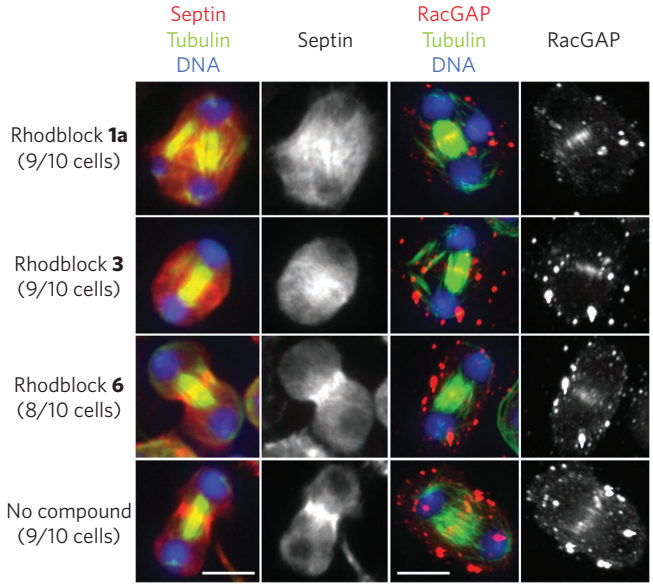

Figure 4 | Effect of Rhodblocks 1a, 3 and 6 on cytokinesis protein localization. The septin Peanut and RacGAP are shown in red in the color-combined figure and again for greater clarity in gray in the neighboring image. Microtubules are shown in green and DNA in blue. Cells were treated with compound for 4 h at the minimally synergistic concentration after overnight Rho RNAi sensitization. The septin Peanut localizes to midzone microtubules in Rhodblock **1a**-treated cells and is partially microtubule-bound and partially diffuse in Rhodblock **3**-treated cells. We analyzed images of ten cells for each condition for Peanut staining. The number of cells represented by the image is shown in parentheses for each compound. RacGAP localization is not perturbed by any Rhodblocks. See **Supplementary Figure 9** for Actin, Rho and Pavarotti staining. The images for each set of markers were taken under identical conditions and were processed identically (see **Supplementary Methods**). Scale bar, 5 μm.

many proteins display functional redundancies, obscuring possible synergistic relationships. We overcame this limitation by performing our screen in *Drosophila* cells, a genetically less complex model system that is useful because many small molecules that are active in *Drosophila* are also active in human cells[29]. For example, RNAi depletion of one of the three human Rho isoforms does not cause cytokinesis failure[30], whereas depletion of the single isoform of *Drosophila* Rho inhibits cytokinesis. Our combination pathway screen has identified several small molecules that target the Rho pathway in *Drosophila* cells. We are now investigating the effects of these small molecules on human cells.

Before this study, three classes of compounds were known to affect the Rho pathway. Rho kinase inhibitors are used in the clinic to treat cardiovascular diseases and have been used as probe compounds to study aspects of the Rho pathway[3,31]. Statins inhibit HMG-CoA reductase (and ultimately cholesterol biosynthesis) and therefore also prevent isoprenylation, which is required for active Rho[31,32]. Although they have been very successful in the clinic as cholesterol-lowering agents, the statins are of limited use in studying the Rho pathway because they affect multiple pathways. Recently, inhibitors of the human formin mDia have been reported[33,34]. In addition to discovering an inhibitor of Rho kinase (Rhodblock **6**), we report several compounds that affect the Rho pathway. These compounds have different phenotypes, indicating that they may have different mechanisms of action and therefore target pathway proteins that have not previously been targeted by a small molecule.

We used myosin phosphorylation as a measure of Rho pathway activity. Interestingly, only one (Rhodblock **6**) of the eight compounds that inhibited myosin phosphorylation inhibited Rok, the protein that is thought to be mainly responsible for MRLC phosphorylation[21,35]. It is likely that some of the Rhodblocks act upstream of Rok, resulting in the downregulation of Rok and therefore in the eventual inhibition of myosin phosphorylation. Rhodblock **1a** is a candidate for upstream action because it causes the mislocalization of several Rho pathway proteins. Rhodblock **3** inhibits the recruitment of phospho-MRLC and Peanut, but not of Anillin or other proteins, and Rhodblock **6** does not significantly inhibit the recruitment to the cleavage furrow of any Rho pathway proteins other than phospho-MRLC. The factors that control the recruitment of myosin to the cleavage furrow and its activation have been the subject of several recent studies[35–37]. There seems to be a consensus that some Rho pathway proteins that are required for active myosin are delivered along interzonal microtubule structures[38,39]. However, it is less clear how these proteins interact to achieve myosin activation. Our compounds prevent the accumulation of phosphorylated myosin at the cleavage furrow while differentially affecting other Rho pathway proteins. We anticipate that the Rhodblocks will be useful in understanding this important aspect of cytokinesis regulation.

Investigations into the role of Rho pathway proteins during cytokinesis and determinants of their localization are active areas of research[30,40–42]. Successful cytokinesis requires that the components of the cytokinetic machinery be properly assembled, organized and maintained at the cleavage furrow. Recent studies indicate that Anillin functions as a key scaffolding protein that brings together other Rho pathway proteins including Rho, RacGAP and pebble as well as actin, myosin and the septin Peanut[26,43–46]. RacGAP interacts with the kinesin-6 protein Pavarotti to make up the Centralspindlin complex, which is crucial for microtubule bundling, central spindle assembly and cytokinesis completion[25]. Therefore, Anillin functions as a molecular bridge that links the actomyosin contractile ring with the Centralspindlin complex and spindle microtubules at the cleavage furrow. A combination of Rhodblock treatments (**Figs. 3**, **4** and **Supplementary Fig. 9**) confirmed a sequential requirement of protein localizations during cytokinesis; that is, myosin localizes independently of actin and Anillin[47] and properly localized RacGAP is needed to localize Anillin, which is needed to localize Septin[26,46]. Rhodblock **3** gives us some insights into the organization of cortical Rho pathway proteins. It mislocalizes phospho-MRLC and septin, but not Anillin, suggesting that Anillin localization is independent of these proteins and that Anillin is an important early component of the furrow.

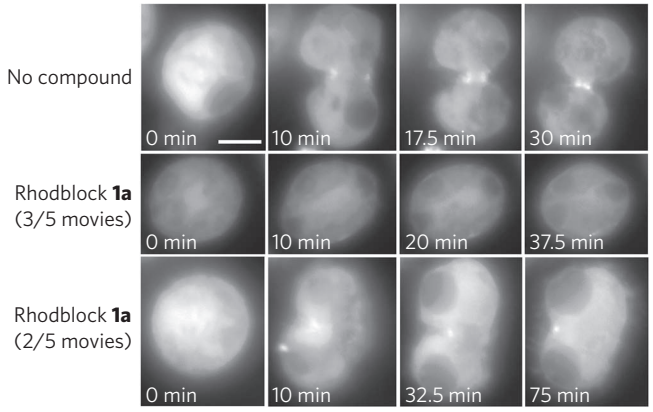

Figure 5 | Movie stills of GFP-MRLC S2 cells treated with 100 μM Rhodblock 1a after overnight Rho RNAi sensitization. In three out of five movies (middle panel), no furrows formed and cells failed to ingress. In two out of five movies (lower panel) a partial furrow formed, briefly ingressed and broke apart. Movie timing was started at the beginning of anaphase. Scale bar (top panel), 5 μm.

Anillin and RacGAP have been shown to interact directly in pull-down and yeast two-hybrid experiments[26,48]. In *Drosophila* embryos, these two proteins are mutually required for localization, and in cultured cells RNAi of RacGAP disrupted Anillin, but not vice versa. As Rhodblock **1a** disrupts Anillin, but not RacGAP, it is likely to target the interaction between RacGAP and Anillin, either directly or by interfering with the regulation of this interaction. Because Rhodblock **1a** is a small molecule that affects its target while it is still present in cells (unlike RNAi, see below), we can use it as a more direct means to dissect the mechanisms regulating the interaction between Anillin and RacGAP50C.

More generally, Rhodblock **1a** perturbed the cortical proteins we tested (actin, Anillin, phospho-MRLC, Peanut and partially Rho), while leaving the Centralspindlin complex unaffected. This means that Rhodblock **1a** disrupts the connection between the cortical and microtubule-bound activities of the Rho pathway, suggesting that microtubule-bound proteins are responsible for the correct delivery of cortical Rho pathway proteins and function upstream in the signaling cascade. This notion is further supported by our live imaging data in GFP-MRLC labeled cells. In some cells, cytokinesis failed without assembly of a furrow, while in other cells a partial furrow briefly formed. Rhodblock **1a** induced additional midzone microtubule bundles that often pointed sharply toward the edge of the cells where the furrow would normally form (**Figs. 3** and **4**). It is possible that cortical Rho pathway proteins are delivered to the furrow along these aberrant bundles, briefly attempt to form a furrow and then dissociate because they are asymmetric or because other ring assembly signals are lacking.

Most of the work from other labs discussed in the previous paragraphs has used RNAi to perturb Rho pathway signaling because few active small molecule inhibitors of the Rho pathway existed. Although there was generally good agreement between reported RNAi experiments and our compound treatments, it is important to keep in mind that small molecule treatments and RNAi can have different effects on cells. RNAi leads to the removal of the target protein, while a small molecule disrupts or inhibits a protein that is still present in the cell[49]. As many Rho-regulated proteins, such as Anillin and the septins, have important scaffolding functions, small molecules that affect these proteins, such as Rhodblocks **1a** or **3**, can be particularly useful because they allow manipulation of protein function without removing the protein. Therefore, as we identify more cellular targets of the Rhodblocks, we anticipate that we will gain further insight into the role of the Rho pathway in cytokinesis and other processes.

In addition to providing interesting and potentially valuable tools with which to study and manipulate the Rho pathway, our pathway screen based on RNAi sensitization is a proof-of-principle study that should be widely applicable to many signaling pathways.

METHODS

Cell culture. *Drosophila* Kc_{167} cells were grown at 25 °C in Schneider's medium (GIBCO) supplemented with 10% heat-inactivated fetal bovine serum (Invitrogen) and penicillin/streptomycin (Cellgro) in T25 and T75 flasks (BD Biosciences).

RNAi-sensitized small molecule screen. Details regarding preparation of double-stranded (ds)RNAs for RNAi treatments are described in the **Supplementary Methods**. On day 1, 6 ml of serum-free Schneider's medium containing 4 μg ml^{-1} Rho dsRNA was added to *Drosophila* Kc_{167} cells grown in T75 flasks at 25 °C. After 1 h, 18 ml of Schneider's medium supplemented with 10% heat-inactivated fetal bovine serum and penicillin/streptomycin was added and cells were incubated for 24 h. On day 2, cells were arrayed in 384-well plates (Costar 3712) at 15,000 cells per well in 40 μl complete growth medium. On day 3, 100 nl of library compounds in DMSO was pin transferred into wells with Rho RNAi-sensitized cells and incubated for 24 h. Cells were then fixed, stained, imaged and analyzed (see below). The screen was performed at the Institute of Chemistry and Cell Biology–Longwood at Harvard Medical School. We screened the known bioactives collection from Biomol, fungal extracts (plates ICBG 2 and 4), the Starr Foundation library, ChemBridge3, ChemDiv5 and ChemDiv4 libraries (http://iccb.med.harvard.edu/screening/compound_libraries/index.htm). For further screening details, see **Supplementary Table 1**. We ordered Rhodblocks **1**–**9**, confirmed their identity and purity (**Supplementary Methods** and **Supplementary Table 6**) and used 10 mM or 50 mM stock solutions in DMSO in subsequent experiments.

Imaging. For screening, cells were fixed and permeabilized in 100 mM Pipes/KOH (pH 6.8), 10 mM EGTA, 1 mM $MgCl_2$, 3.7% formaldehyde and 0.2% TritonX-100 for 15 min and then washed in PBS. Whole cells were stained with 0.5 μg ml^{-1} NHS-tetramethylrhodamine (5-[and-6]-carboxytetramethylrhodamine, succinimidyl ester C; Molecular Probes) in PBS. DNA was stained with 5 μg ml^{-1} Hoechst 33342 in TBST (TBS with 1% TritonX-100) for 15 min. Cells were then washed twice with TBST and sealed with aluminum seals (Costar) for image acquisition[50]. Cells were imaged using the ImageXpress Micro (Molecular Devices) at ICCB-Longwood using the ×20 objective.

For spinning disk confocal microscopy, cells were grown on glass coverslips and were fixed and permeabilized as above. Cells were blocked in AbDil (TBST with 2% BSA) for 30 min and stained at 4 °C overnight with one of the following antibodies diluted in AbDil: anti–phospho myosin light chain-2 (3671S, Cell Signaling), anti-Anillin, anti-Peanut (gifts from C. Field, Harvard Medical School), anti-Rho (p1D9; Iowa Hybridoma Bank), anti-RacGAP50C (a gift from R. Saint, Australian National University) and anti-Pavarotti. The antibody to Pavarotti was raised in rabbits using the C-terminal peptide CNLGIEGHSSKKSKI. Actin was stained with tetramethylrhodamine isothiocyanate–phalloidin (P1951, Sigma). Cells were washed with TBST and stained for 2 h with secondary antibodies (for example, 1:1,000 goat anti-rabbit– or anti-rat–Alexa Fluor 594 (Invitrogen)) followed by 2 h with 1:2,000 fluorescein isothiocyanate–labeled anti-tubulin (DM1alpha, Sigma) in AbDil. The DNA was stained with 5 μg ml^{-1} Hoechst 33342 in TBST for 15 min followed by two TBST washes. Coverslips were mounted on glass slides using ProLong Gold (Invitrogen). Details regarding confocal image acquisition and linescan analysis are described in the **Supplementary Methods**.

For live-cell imaging, cells were allowed to attach on 25-mm round no. 1.5 glass coverslips (64-0715, Warner Instruments) for 1 h before imaging. S2 cells expressing GFP fused to myosin regulatory light chain were a gift from E. Griffis, University of California, San Francisco[39]. Myosin-GFP images were collected every 2.5 min with a Nikon TE2000E microscope equipped with a ×100 Plan Apo, numerical aperture 1.4 objective lens.

RNAi of Rho pathway proteins. For **Table 1**, cells were sensitized with a 1-day RNAi treatment (as described above) of Rho pathway proteins (RhoA, pebble, RacGAP50C, Diaphanous, Citron kinase, Rho kinase at 4, 1, 5, 16, 1 and 16 μg ml^{-1} dsRNA, respectively), followed by a 24-h small molecule treatment (2 d total RNAi treatment). In the localization experiments in **Figures 3** and **4** and **Supplementary Figure 9**, control and RNAi-sensitized cells were treated for 4 h with compound. For double RNAi treatments, 10 μg ml^{-1} Dia dsRNA was used.

Synergy ratios. The synergy ratio in **Table 1** is defined by Equation (1), where the observed phenotype refers to the percentage of binucleate cells experimentally measured after combined small molecule and RNAi treatment (Φ_{ab}), while the expected phenotype refers to the expected percentage of binucleate cells after combined treatment assuming a multiplicative model where small molecule (Φ_a) and RNAi treatments (Φ_b) are statistically independent. The background level of binucleate cells present in the untreated controls has been subtracted from all treatment values (indicated by the prime symbol).

$$\text{Synergy ratio} = \frac{\text{observed phenotype}}{\text{expected phenotype}} = \frac{\Phi'_{ab}}{1-\left(1-\Phi'_a\right)\left(1-\Phi'_b\right)} \quad (1)$$

A synergy ratio of 1 indicates that there is no synergy between the small molecule and RNAi treatments. If there is synergy—that is, cooperative effects between the two treatments—the incidence of binucleate cells should be higher than expected in a multiplicative model of individual treatments' background levels, reflected in a synergy ratio greater than 1. A synergy ratio less than 1 indicates that one treatment suppresses the effects of the other. The maximum possible synergy ratio depends on the level of individual action. To allow a large range of synergy ratios, we set the experimental conditions reflected in **Table 1** so that the individual actions were small.

Rho kinase assay. To obtain *Drosophila* Rho kinase, subconfluent *Drosophila* Kc_{167} cells in T75 flasks were transiently transfected with 40 μg full-length Rok-pAFW (FLAG plasmid pAFW was obtained from the Drosophila Gateway Collection) and expressed for 3 d. Rok-FLAG was then purified by immunoprecipitation from cell lysates using Anti-FLAG M2 agarose (Sigma). Aliquots of kinase were snap frozen and stored at −20 °C. For the kinase assay, compounds were incubated with Rok-FLAG and myelin basic protein (MBP) substrate in kinase buffer (20 mM Tris, 1 mM $MgCl_2$, 25 mM KCl, 1 mM DTT, 0.04 mg ml^{-1} BSA). After 15 min, the kinase reaction was initiated by the addition of ATP (100 μM final) including approximately 0.3 μCi μl^{-1} [γ-^{32}P]ATP. Reactions were performed in a total volume of 20 μl. After 10 min, the reaction was terminated by spotting 17.5 μl of the reaction mixture on P81-phosphocellulose paper (diameter 2.1 cm, Whatman). P81 circles

were then washed four times (5 min each) with 0.75% phosphoric acid, once with acetone and dried. Radioactivity was then measured by liquid scintillation counting.

Received 19 November 2009; accepted 22 March 2010; published online 2 May 2010

References

1. Jaffe, A.B. & Hall, A. Rho GTPases: biochemistry and biology. *Annu. Rev. Cell Dev. Biol.* **21**, 247–269 (2005).
2. Gomez del Pulgar, T., Benitah, S.A., Valeron, P.F., Espina, C. & Lacal, J.C. Rho GTPase expression in tumourigenesis: evidence for a significant link. *Bioessays* **27**, 602–613 (2005).
3. Budzyn, K., Marley, P.D. & Sobey, C.G. Targeting Rho and Rho-kinase in the treatment of cardiovascular disease. *Trends Pharmacol. Sci.* **27**, 97–104 (2006).
4. Fritz, G., Brachetti, C., Bahlmann, F., Schmidt, M. & Kaina, B. Rho GTPases in human breast tumours: expression and mutation analyses and correlation with clinical parameters. *Br. J. Cancer* **87**, 635–644 (2002).
5. Fritz, G., Just, I. & Kaina, B. Rho GTPases are over-expressed in human tumors. *Int. J. Cancer* **81**, 682–687 (1999).
6. Sahai, E. & Marshall, C.J. RHO-GTPases and cancer. *Nat. Rev. Cancer* **2**, 133–142 (2002).
7. Benitah, S.A., Valeron, P.F., van Aelst, L., Marshall, C.J. & Lacal, J.C. Rho GTPases in human cancer: an unresolved link to upstream and downstream transcriptional regulation. *Biochim. Biophys. Acta* **1705**, 121–132 (2004).
8. Eggert, U.S., Mitchison, T.J. & Field, C.M. ANIMAL CYTOKINESIS: From Parts List to Mechanisms. *Annu. Rev. Biochem.* **75**, 543–566 (2006).
9. Walker, K. & Olson, M.F. Targeting Ras and Rho GTPases as opportunities for cancer therapeutics. *Curr. Opin. Genet. Dev.* **15**, 62–68 (2005).
10. Aznar, S., Fernandez-Valeron, P., Espina, C. & Lacal, J.C. Rho GTPases: potential candidates for anticancer therapy. *Cancer Lett.* **206**, 181–191 (2004).
11. Sprang, S.R. G protein mechanisms: insights from structural analysis. *Annu. Rev. Biochem.* **66**, 639–678 (1997).
12. Doe, C. *et al.* Novel Rho kinase inhibitors with anti-inflammatory and vasodilatory activities. *J. Pharmacol. Exp. Ther.* **320**, 89–98 (2007).
13. Carpenter, A.E. *et al.* CellProfiler: image analysis software for identifying and quantifying cell phenotypes. *Genome Biol.* **7**, R100 (2006).
14. Jones, T.R. *et al.* Scoring diverse cellular morphologies in image-based screens with iterative feedback and machine learning. *Proc. Natl. Acad. Sci. USA* **106**, 1826–1831 (2009).
15. Genth, H. *et al.* Entrapment of Rho ADP-ribosylated by Clostridium botulinum C3 exoenzyme in the Rho-guanine nucleotide dissociation inhibitor-1 complex. *J. Biol. Chem.* **278**, 28523–28527 (2003).
16. Somers, W.G. & Saint, R.A. RhoGEF and Rho family GTPase-activating protein complex links the contractile ring to cortical microtubules at the onset of cytokinesis. *Dev. Cell* **4**, 29–39 (2003).
17. Hirose, K., Kawashima, T., Iwamoto, I., Nosaka, T. & Kitamura, T. MgcRacGAP is involved in cytokinesis through associating with mitotic spindle and midbody. *J. Biol. Chem.* **276**, 5821–5828 (2001).
18. Maddox, A.S. & Oegema, K. Closing the GAP: a role for a RhoA GAP in cytokinesis. *Mol. Cell* **11**, 846–848 (2003).
19. Prokopenko, S.N. *et al.* A putative exchange factor for Rho1 GTPase is required for initiation of cytokinesis in *Drosophila*. *Genes Dev.* **13**, 2301–2314 (1999).
20. Watanabe, N. *et al.* p140mDia, a mammalian homolog of *Drosophila* diaphanous, is a target protein for Rho small GTPase and is a ligand for profilin. *EMBO J.* **16**, 3044–3056 (1997).
21. Hickson, G.R., Echard, A. & O'Farrell, P.H. Rho-kinase controls cell shape changes during cytokinesis. *Curr. Biol.* **16**, 359–370 (2006).
22. Zavortink, M., Contreras, N., Addy, T., Bejsovec, A. & Saint, R. Tum/RacGAP50C provides a critical link between anaphase microtubules and the assembly of the contractile ring in *Drosophila melanogaster*. *J. Cell Sci.* **118**, 5381–5392 (2005).
23. Hall, A. Rho GTPases and the control of cell behaviour. *Biochem. Soc. Trans.* **33**, 891–895 (2005).
24. Matsumura, F. Regulation of myosin II during cytokinesis in higher eukaryotes. *Trends Cell Biol.* **15**, 371–377 (2005).
25. Mishima, M., Kaitna, S. & Glotzer, M. Central spindle assembly and cytokinesis require a kinesin-like protein/RhoGAP complex with microtubule bundling activity. *Dev. Cell* **2**, 41–54 (2002).
26. D'Avino, P.P. *et al.* Interaction between Anillin and RacGAP50C connects the actomyosin contractile ring with spindle microtubules at the cell division site. *J. Cell Sci.* **121**, 1151–1158 (2008).
27. Lehar, J., Stockwell, B.R., Giaever, G. & Nislow, C. Combination chemical genetics. *Nat. Chem. Biol.* **4**, 674–681 (2008).
28. Wang, J. *et al.* Platensimycin is a selective FabF inhibitor with potent antibiotic properties. *Nature* **441**, 358–361 (2006).
29. Perrimon, N., Friedman, A., Mathey-Prevot, B. & Eggert, U.S. Drug-target identification in *Drosophila* cells: combining high-throughout RNAi and small-molecule screens. *Drug Discov. Today* **12**, 28–33 (2007).
30. Kamijo, K. *et al.* Dissecting the role of Rho-mediated signaling in contractile ring formation. *Mol. Biol. Cell* **17**, 43–55 (2006).
31. Ishizaki, T. *et al.* Pharmacological properties of Y-27632, a specific inhibitor of rho-associated kinases. *Mol. Pharmacol.* **57**, 976–983 (2000).
32. Liao, J.K. & Laufs, U. Pleiotropic effects of statins. *Annu. Rev. Pharmacol. Toxicol.* **45**, 89–118 (2005).
33. Rizvi, S. A. *et al.* Identification and characterization of a small molecule inhibitor of formin-mediated actin assembly. *Chem Biol* **16**, 1158–1168 (2009).
34. Gauvin, T.J., Fukui, J., Peterson, J.R. & Higgs, H.N. Isoform-selective chemical inhibition of mDia-mediated actin assembly. *Biochemistry* **48**, 9327–9329 (2009).
35. Dean, S.O. & Spudich, J.A. Rho kinase's role in myosin recruitment to the equatorial cortex of mitotic *Drosophila* S2 cells is for myosin regulatory light chain phosphorylation. *PLoS One* **1**, e131 (2006).
36. Dean, S.O., Rogers, S.L., Stuurman, N., Vale, R.D. & Spudich, J.A. Distinct pathways control recruitment and maintenance of myosin II at the cleavage furrow during cytokinesis. *Proc. Natl. Acad. Sci. USA* **102**, 13473–13478 (2005).
37. Murthy, K. & Wadsworth, P. Myosin-II-dependent localization and dynamics of F-actin during cytokinesis. *Curr. Biol.* **15**, 724–731 (2005).
38. Foe, V.E. & von Dassow, G. Stable and dynamic microtubules coordinately shape the myosin activation zone during cytokinetic furrow formation. *J. Cell Biol.* **183**, 457–470 (2008).
39. Vale, R.D., Spudich, J.A. & Griffis, E.R. Dynamics of myosin, microtubules, and Kinesin-6 at the cortex during cytokinesis in *Drosophila* S2 cells. *J. Cell Biol.* **186**, 727–738 (2009).
40. Miller, A.L. & Bement, W.M. Regulation of cytokinesis by Rho GTPase flux. *Nat. Cell Biol.* **11**, 71–77 (2009).
41. Mishima, M. & Glotzer, M. Cytokinesis: a logical GAP. *Curr. Biol.* **13**, R589–R591 (2003).
42. Piekny, A., Werner, M. & Glotzer, M. Cytokinesis: welcome to the Rho zone. *Trends Cell Biol.* **15**, 651–658 (2005).
43. Piekny, A.J. & Glotzer, M. Anillin is a scaffold protein that links RhoA, actin, and myosin during cytokinesis. *Curr. Biol.* **18**, 30–36 (2008).
44. D'Avino, P.P. How to scaffold the contractile ring for a safe cytokinesis—lessons from Anillin-related proteins. *J. Cell Sci.* **122**, 1071–1079 (2009).
45. Hickson, G.R. & O'Farrell, P.H. Anillin: a pivotal organizer of the cytokinetic machinery. *Biochem. Soc. Trans.* **36**, 439–441 (2008).
46. Hickson, G.R. & O'Farrell, P.H. Rho-dependent control of anillin behavior during cytokinesis. *J. Cell Biol.* **180**, 285–294 (2008).
47. Straight, A.F., Field, C.M. & Mitchison, T.J. Anillin binds nonmuscle myosin II and regulates the contractile ring. *Mol. Biol. Cell* **16**, 193–201 (2005).
48. Gregory, S.L. *et al.* Cell division requires a direct link between microtubule-bound RacGAP and Anillin in the contractile ring. *Curr. Biol.* **18**, 25–29 (2008).
49. Eggert, U.S., Field, C.M. & Mitchison, T.J. Small molecules in an RNAi world. *Mol. Biosyst.* **2**, 93–96 (2006).
50. Eggert, U.S. *et al.* Parallel chemical genetic and genome-wide RNAi screens identify cytokinesis inhibitors and targets. *PLoS Biol.* **2**, e379 (2004).

Acknowledgments

We thank the staff at ICCB-Longwood, the Nikon Imaging Center at Harvard Medical School and the Broad Institute's Imaging Platform for their assistance and F. Roth for helpful discussions. We thank C. Field (Harvard Medical School), R. Saint (Australian National University) and E. Griffis (University of California, San Francisco) for reagents. Funding for M.S.V., T.R.J. and A.E.C. was from the Life Sciences Research Foundation (Novartis), L'Oreal for Women in Science, the Society for Biomolecular Screening and the US National Institutes of Health (NIH) 5 RL1 CA133834-03. A.B.C., Y.S., A.D.T. and U.S.E. were supported by NIH grant R01 GM082834, the Claudia Adams Barr Program and the Dana-Farber Cancer Institute.

Author contributions

A.B.C. and U.S.E. designed the study. A.B.C., Y.S., A.D.T. and U.S.E. designed and conducted experiments and analyzed data. A.B.C., Y.S., M.S.V., T.R.J. and A.E.C. designed and performed automated image analysis. U.S.E. wrote the manuscript, with input from the other authors.

Competing financial interests

The authors declare no competing financial interests.

Additional information

Supplementary information and chemical compound information are available online at http://www.nature.com/naturechemicalbiology/. Reprints and permissions information is available online at http://npg.nature.com/reprintsandpermissions/. Correspondence and requests for materials should be addressed to U.S.E.

Supplementary Information

Small molecules discovered in a pathway screen target the Rho pathway in cytokinesis

Adam B. Castoreno,[1] Yegor Smurnyy,[1] Angelica D. Torres,[1] Martha S. Vokes,[2] Thouis R. Jones,[2] Anne E. Carpenter[2] and Ulrike S. Eggert[1,*]

[1]Dana-Farber Cancer Institute and Department of Biological Chemistry and Molecular Pharmacology, Harvard Medical School, Boston, Massachusetts 02115 and [2]The Broad Institute of Harvard and MIT, Cambridge, Massachusetts 02142.

Nature Chemical Biology: doi: 10.1038/nchembio.363

Supplementary methods

RNAi constructs

Double-stranded (ds)RNAs for RNAi experiments were transcribed *in vitro* using the MEGAscript T7 kit (Ambion) and purified with RNAeasy columns (Qiagen). cDNA templates contained the T7 promoter sequence (TAATACGACTCACTATAGGG) and were amplified from *Drosophila* Kc_{167} genomic DNA with Herculase (Stratagene) and the following primer pairs (each primer contained the T7 promoter sequence added to the 5' end):

Rho1 5'-GACGACGATTCGCAAGAAAT-3' and 5'-CTCGATGTCGGCCACATAAT-3'

Pbl 5'-TTTTAAAAACAAGTTGGAAGAGTT-3' and 5'-CCATGCGCGATTCGGT-3'

RacGAP50C 5'- CGATGTGCGCACATCAAA-3' and 5'- TGACACTGAACGCAATTGTC-3'

Citron kinase 5'- AAATGTGGTCCAAGAAGGAAG-3' and 5'- GAGGCGATCTCCTCGTTC-3'

Rok 5'-GCTCGGCCAGGAGAATG-3' and 5'-CAGAGCGGCCACCTTC-3'

Dia 5'-GGTCGGAGGAGTACGAGA-3' and 5'-AATGCCTTGTCGGACATTTT-3'

Ial 5'- GCCATGAAGGTGATGTTCAAA-3' and 5'- CAGCCGACGACGAACTC-3'

Tsr 5'- TGGTGTAACTGTGTCTGATGT-3' and 5'- CATTTCTGGATATCTTCTAGAAAC-3'

Mbs 5'=ACGAAACAAGCTCTGCATC-3' and 5'-AGGATGATTTGATAGCTTCTGT-3'

Confocal Image Acquisition and Linescan Analysis

Images were collected with a Yokogawa spinning disk confocal on a Nikon Ti inverted microscope equipped with a 100x Plan Apo NA 1.4 objective lens. To eliminate any bias toward identifying mislocalization phenotypes, cells in early stage cytokinesis were selected based on microtubules. Images were acquired with a Hamamatsu ORCA ER cooled CCD camera controlled with MetaMorph 7 software. Z-series optical sections were collected with a step size of 0.3 microns. Images were processed using MetaMorph 7 software. Filter, mirror and laser configurations are listed on the Nikon Image Center at the Harvard Medical School website (https://nic.med.harvard.edu/). Maximum projections are shown in Fig. 3 and sum (for septin) and maximum (for RacGAP) projections in Fig. 4.

Nature Chemical Biology: doi: 10.1038/nchembio.363

The fluorescence intensity of Anillin, phospho-MRLC and Rho were analyzed using the Linescan function in MetaMorph using sum projections generated from image stacks. Briefly, a line 10 microns long and 5 pixels wide was drawn across the cleavage furrow using Anillin or Rho as a guide. In the case where cytokinesis proteins were mislocalized, the line was placed perpendicular to the center of the interzonal microtubules. For each point along the line, the average intensity of the 5 pixels was calculated in MetaMorph and transferred to Microscoft Excel and graphed as average intensity *vs.* distance in micrometers as shown in Fig. 3 and Supplementary Fig. 8.

RNAi optimization

To optimize partial Rho RNAi conditions, several parameters were varied, including the sequence and concentration of the dsRNA and length of RNAi treatment. The timing of RNAi treatment (**Supplementary Fig. 1**) was the most critical. Optimal conditions are described in the general methods section.

Automated Image Analysis (Supplementary Fig. 4)

We used CellProfiler software to automatically score our screening data. Images are first processed with CellProfiler, which identifies individual cells, nuclei and cytoplasms (*i.e.* cells minus nuclei) and measures their geometric characteristics, staining intensity and texture. Measurements are done independently for each channel and each cellular compartment, with object outlines overlaid onto initial images and the result saved separately. To improve the quality of the output, an additional module identifies cells that might be detected incorrectly due to distorted shape or heavy clumping and marks them by a different color of the cell outline; such cells can be included in the subsequent analysis at the user's discretion. In addition, measurements are saved in a tab-delimited text file and imported into a MySQL database. In the next stage, a supervised machine learning system (the Classifier feature of CellProfiler Analyst) is used to distinguish between mono- and binucleate cells and score individual images. Typically, a user is presented with cells, either selected randomly from the array or taken from a specific plate with positive or negative controls. Cells of either phenotypic class are manually picked and, after enough examples are acquired, machine learning algorithms are able to select certain measurements that can distinguish between two classes. The procedure is repeated

Nature Chemical Biology: doi: 10.1038/nchembio.363

several times, until 10-15 key measurements are selected and phenotype classification is robust enough. After that the software scores all available images and presents the data for final manual verification and follow up.

In addition to CellProfiler analysis, we also used analysis modules in the Molecular Devices MetaXpress software to quantify binucleate cells.

Control small molecule/RNAi treatments

We determined the synergy ratios for three known inhibitors of the Rho pathway (**Supplementary Table 4**): Rho kinase inhibitor GSK269962A, the protein inhibitor of Rho CT04 and Lovastatin (Calbiochem #438185). Cells were sensitized with a 1 day RNAi treatment of Rho pathway proteins (RhoA, Pebble, RacGAP50C, Diaphanous, Citron kinase, Rho kinase), followed by a 24 h small molecule treatment (2 day total RNAi treatment).

In addition to the constructs shown in Table 1, we also treated Rho RNAi-sensitized cells with dsRNA corresponding to ial (*Drosophila* Aurora B) and tsr (*Drosophila* cofilin). Both proteins are involved in cytokinesis, but not central to the Rho pathway and did not show significant synergy with Rho RNAi. We also tested other small molecule inhibitors of cytokinesis available in our lab (from Eggert *et al.* PLoS Biology 2004). Binucleines 3, 4, 9 and 12 at 50 μM did not show significant synergy with Rho RNAi.

Small molecule analysis

We reordered the Rhodblocks from ChemBridge or ChemDiv and confirmed their purity and identity by NMR and LCMS (see Supplementary Table 6 for LCMS traces and ordering information).

Rhodblock 1a: ^{1}H NMR (600 MHz, d6-DMSO): δ 7.85-7.87 (m, 2H), 7.49-7.52 (m, 2H), 7.32-7.35 (m, 4H), 7.22-7.27 (m, 4H), 6.73 (t, J = 2.1 Hz, 1H), 5.74 (q, J = 12 Hz, 1H), 3.92 (q, J = 18 Hz, 1H), 3.19 (q, J = 17 Hz, 1H), 2.49-2.51 (m, 1H); ^{13}C NMR (150 MHz, d6-DMSO): δ 156.7, 155.4, 146.8, 146.4, 142.8, 131.6, 131.3, 129.6, 129.4, 128.0, 126.2, 119.7, 112.7, 61.3, 41.8; MS (*m/z*): $[M+H]^{+}$ calcd. for $C_{20}H_{17}N_2O_2$, 317.12; found, 316.87.

Rhodblock 1b: ^{1}H NMR (600 MHz, d6-DMSO): δ 7.80-7.82 (m, 2H), 7.28-7.30 (m, 2H), 7.09 (d, J = 9 Hz, 2H), 6.85 (d, J = 9 Hz, 2H), 5.46 (q, J = 12 Hz, 1H), 3.70 (s, 3H), 3.08 (q, J = 18 Hz, 2H), 2.67-2.70 (m, 2H), 1.03 (t, J = 7 Hz, 3H); ^{13}C NMR (150 MHz, d6-DMSO): δ 183.6,

Nature Chemical Biology: doi: 10.1038/nchembio.363

171.1, 159.1, 153.8, 135.2, 129.6, 128.6, 127.4, 116.4, 114.7, 59.8, 55.8, 42.6, 27.6, 9.7; MS (*m/z*): $[M+H]^+$ calcd. for $C_{19}H_{20}FN_2O_2$, 327.14; found, 326.86.

Rhodblock 2: ^1H NMR (600 MHz, d6-DMSO): δ 10.79 (s, 1H), 7.76-7.82 (m, 3H), 7.67-7.69 (m, 2H), 7.46-7.51 (m, 4H), 2.77 (q, J = 7 Hz, 2 H), 2.60 (s, 3H), 0.97 (t, J = 7 Hz, 3H); ^{13}C NMR (150 MHz, d6-DMSO): δ 171.1, 161.1, 161.0, 142.6, 130.9, 129.6, 128.6, 128.5, 128.4, 124.8, 120.2, 113.7, 38.2, 15.4, 12.7; MS (*m/z*): $[M+H]^+$ calcd. for $C_{19}H_{20}N_3O_4S$, 386.11; found, 385.80.

Rhodblock 3: ^1H NMR (600 MHz, d6-DMSO): δ 7.81 (s, 1H), 7.68 (s, 1H), 7.57 (s, 1H), 7.00 (s, 2H), 3.45 (d, J = 1.2 Hz, 2H), 2.41 (s, 3H); ^{13}C NMR (150 MHz, d6-DMSO): δ 171.8, 154.0, 144.7, 132.0, 128.4, 128.1, 120.6, 115.4, 113.9, 30.9, 20.8; MS (*m/z*): $[M+H]^+$ calcd. for $C_{11}H_{11}ClNO_2$, 224.04; found, 223.90.

Rhodblock 4: ^1H NMR (600 MHz, d6-DMSO): δ 7.96 (s, 1H), 7.78-7.79 (m, 2H), 7.57-7.59 (m, 1H), 7.51-7.53 (m, 1H), 7.33-7.34 (m, 1H), 7.22-7.25 (m, 1H), 3.87 (s, 2H), 3.44 (q, J = 7 Hz, 1H), 1.22 (d, J = 7 Hz, 3H); ^{13}C NMR (150 MHz, d6-DMSO): δ 175.6, 144.4, 143.4, 141.7, 138.7, 136.9, 127.4, 126.7, 125.7, 120.8, 120.1, 118.6, 116.6, 51.8, 37.2, 22.2; MS (*m/z*): $[M+H]^+$ calcd. for $C_{16}H_{17}N_2O$, 253.13; found, 252.93.

Rhodblock 5: ^1H NMR (600 MHz, d6-DMSO): δ 7.61-7.64 (m, 2H), 7.25 (d, J = 9 Hz, 1H), 7.00 (s, 1H), 4.20 (q, J = 7 Hz, 2H), 2.45 (d, J = 4.8 Hz, 3H), 1.33 (t, J = 7 Hz, 3H); ^{13}C NMR (150 MHz, d6-DMSO): δ 155.1, 134.5, 129.7, 129.4, 124.2, 116.5, 65.5, 29.5, 14.8; MS (*m/z*): $[M+H]^+$ calcd. for $C_9H_{13}N_2ClSO_3$, 250.02; found, 249.85.

Rhodblock 6: ^1H NMR (600 MHz, d6-DMSO): δ 12.93 (s, 1H), 9.69 (s, 1H), 8.14 (s, 1H), 8.00 (s, 1H), 7.42-7.47 (m, 1H), 3.21-3.27 (m, 1H), 2.22-2.30 (m, 4H), 2.10-2.14 (m, 2H); ^{13}C NMR (150 MHz, d6-DMSO): δ 173.3, 134.0, 133.1, 121.1, 110.7, 110.2, 25.4, 18.5; MS (*m/z*): $[M+H]^+$ calcd. for $C_{12}H_{14}N_3O$, 216.11; found, 215.99.

Rhodblock 7: ^1H NMR (600 MHz, d6-DMSO): δ 7.82 (d, J = 8 Hz, 2H), 7.47 (d, J = 8 Hz, 2H), 7.00 (s, 1H), 3.55 (d, J = 6 Hz, 2H), 3.26 (d, J = 6 Hz, 2H), 2.01-2.03 (m, 1H), 1.84-1.86 (m, 1H), 0.88 (d, J = 6 Hz, 6H), 0.75 (d, J = 6 Hz, 6H); ^{13}C NMR (150 MHz, d6-DMSO): δ 129.6, 127.6, 104.8, 55.9, 53.2, 27.8, 26.8, 20.7, 20.3; MS (*m/z*): $[M+H]^+$ calcd. for $C_{18}H_{25}ClN_3O$, 334.16; found, 333.91.

Rhodblock 8: ^1H NMR (600 MHz, d6-DMSO): δ 11.39 (s, 2H), 8.16 (s, 1H), 8.00 (s, 1H), 7.72 (d, J = 6 Hz, 2H), 7.26 (d, J = 6 Hz, 2H), 2.50 (s, 3H); ^{13}C NMR (150 MHz, d6-DMSO): δ 178.5, 142.5, 141.3, 131.4, 128.4, 126.2, 15.0; MS (*m/z*): $[M+H]^+$ calcd. for $C_9H_{12}N_3S_2$, 226.04; found, 225.91.

Nature Chemical Biology: doi: 10.1038/nchembio.363

Supplementary figures

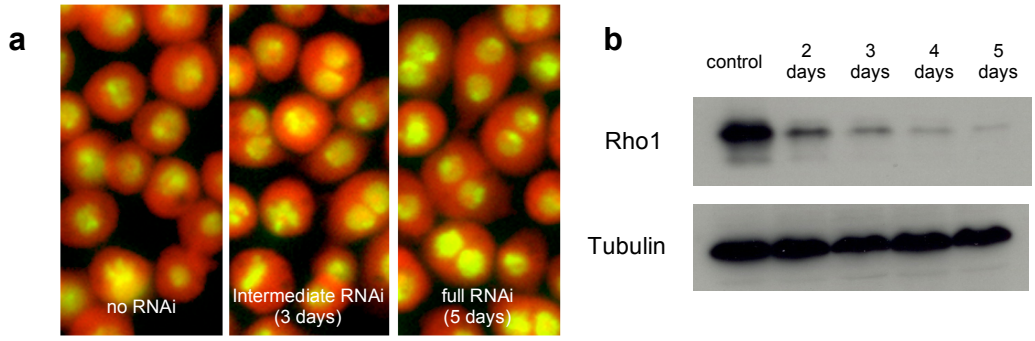

Supplementary Figure 1 (a) *Example of intermediate and full RNAi phenotypes.* Note how the percentage of binucleate cells increases in the 5 day vs. 3 day treatments. (*Drosophila* Kc_{167} cells are shown in red, DNA in yellow). **(b)** *Western blot of Rho1*. The decreasing levels of Rho1 over time correlate with the percentage of binucleate cells. Tubulin is shown as a loading control. Cell lysates were separated by 12% SDS PAGE, transferred to nitrocellulose and blotted using anti-Rho or anti-tubulin).

Nature Chemical Biology: doi: 10.1038/nchembio.363

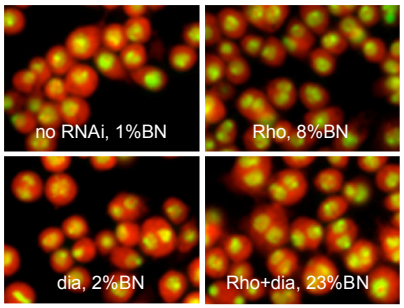

Supplementary Figure 2 *Example of synergy between RNAi of different Rho pathway proteins*. Note how the percentage of binucleate cells (% BN, calculated from ~ 3000 cells) increases substantially when cells are treated with two RNAi constructs targeting different proteins within the pathway. (*Drosophila* Kc_{167} cells are shown in red, nuclei in yellow).

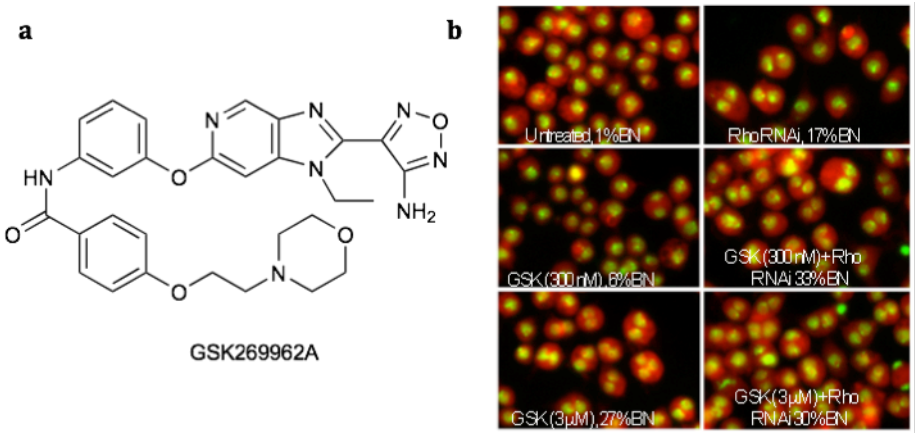

Supplementary Figure 3 *Synergy between GSK269962A and Rho RNAi.* Note that GSK269962A does not inhibit cytokinesis at 300 nM, but strongly synergizes with Rho RNAi. As predicted by our screening concept, GSK269962A inhibits cytokinesis at higher concentrations (3 μM) in the absence of Rho RNAi (*Drosophila* Kc_{167} cells are shown in red, nuclei in yellow).

Nature Chemical Biology: doi: 10.1038/nchembio.363

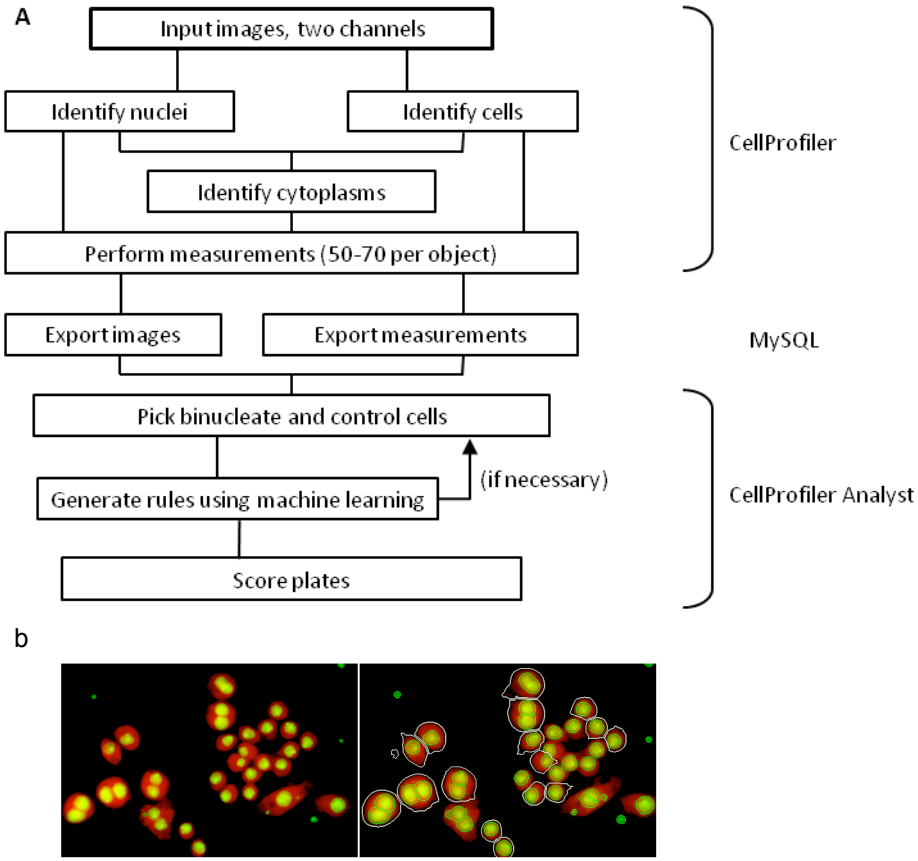

Supplementary Figure 4 (a) *Overview of the automatic processing pipeline.* See the supplementary methods for details. **(b)** *Sample image, before and after processing with the pipeline*. Whole cell staining in red, nuclei in green. On the right, the image with overlaid outlines of regular cells (white) and nuclei (green), cells that were likely misidentified are not outlined.

Nature Chemical Biology: doi: 10.1038/nchembio.363

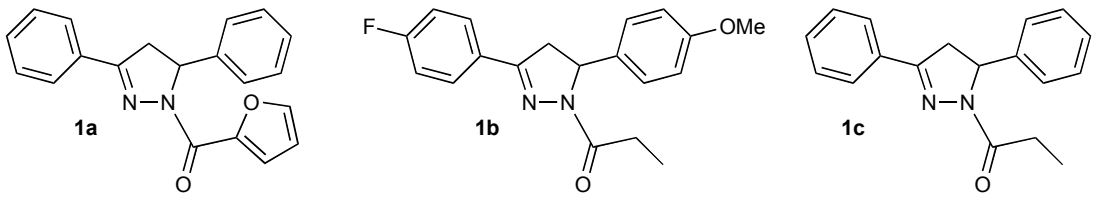

Supplementary Figure 5 *Chemical structures of Rhodblocks **1a-c**.*

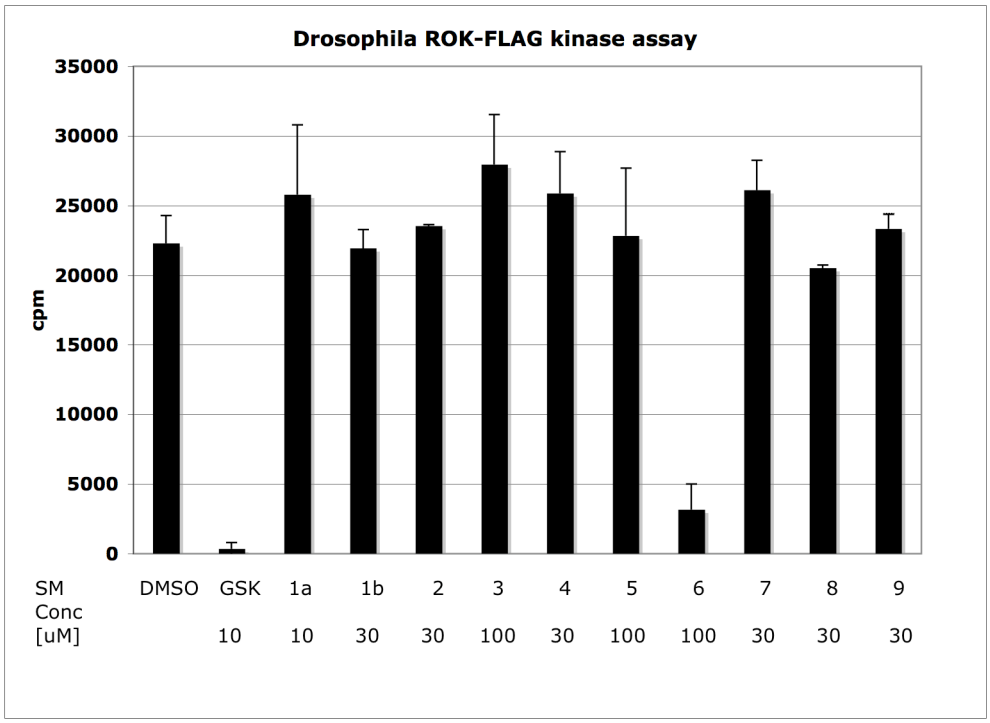

Supplementary Figure 6 *Drosophila* Rho kinase assay data for all Rhodblocks. Error bars indicate standard deviation (n=2).

Nature Chemical Biology: doi: 10.1038/nchembio.363

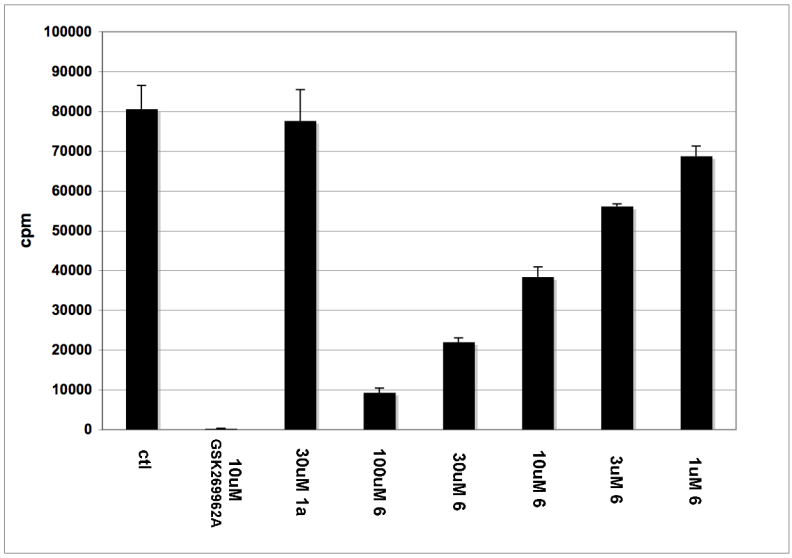

Supplementary Figure 7. *Rho kinase (human ROCK I) assay data for Rhodblock* ***6***. A dose-response curve is shown as well as control data for the Rho kinase inhibitor GSK269962A and Rhodblock **1a**. The kinase assay was performed as described in the Methods for Drosophila Rok, but human ROCK 1 (Invitrogen, PV3691) was used instead. Error bars indicate standard deviation (n=2).

Nature Chemical Biology: doi: 10.1038/nchembio.363

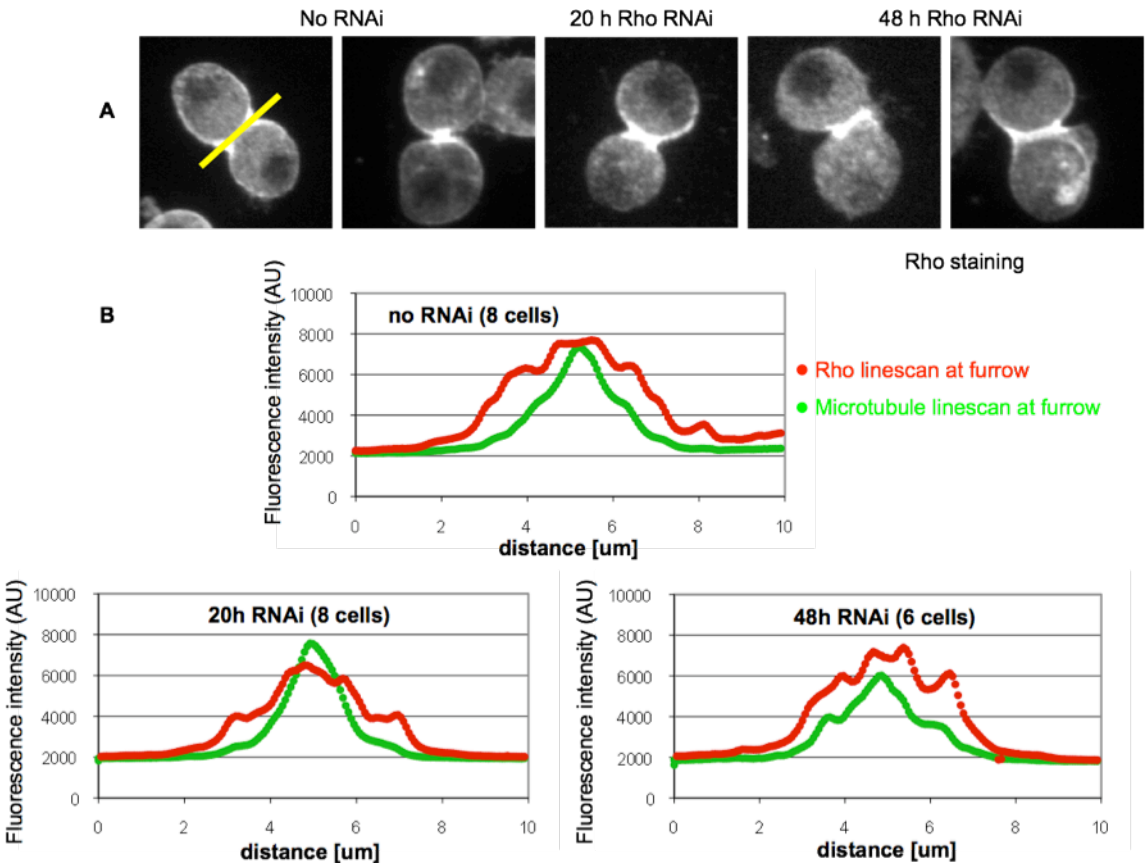

Supplementary Figure 8 *Rho localizations after short Rho RNAi treatments.* To amplify the effects of our Rhodblock compounds, we sensitize cells by overnight Rho RNAi treatments. The top panel in this figure shows Rho staining in cells at different stages of cytokinesis treated with Rho dsRNA for 0, 20 or 48 h. The lower panels show averaged linescans quantitating Rho fluorescence intensity at the furrow for each time point. Note that there is not a significant reduction in average Rho fluorescence intensity at the furrow after 48 h RNAi. In lower resolution images, we also identified 50 cytokinetic cells for each time point using tubulin staining. We then looked at Rho staining and found that 50/50 cells at 0 h and 20 h and 46/50 cells at 48 h RNAi had correct Rho localization at the cleavage furrow.

Nature Chemical Biology: doi: 10.1038/nchembio.363

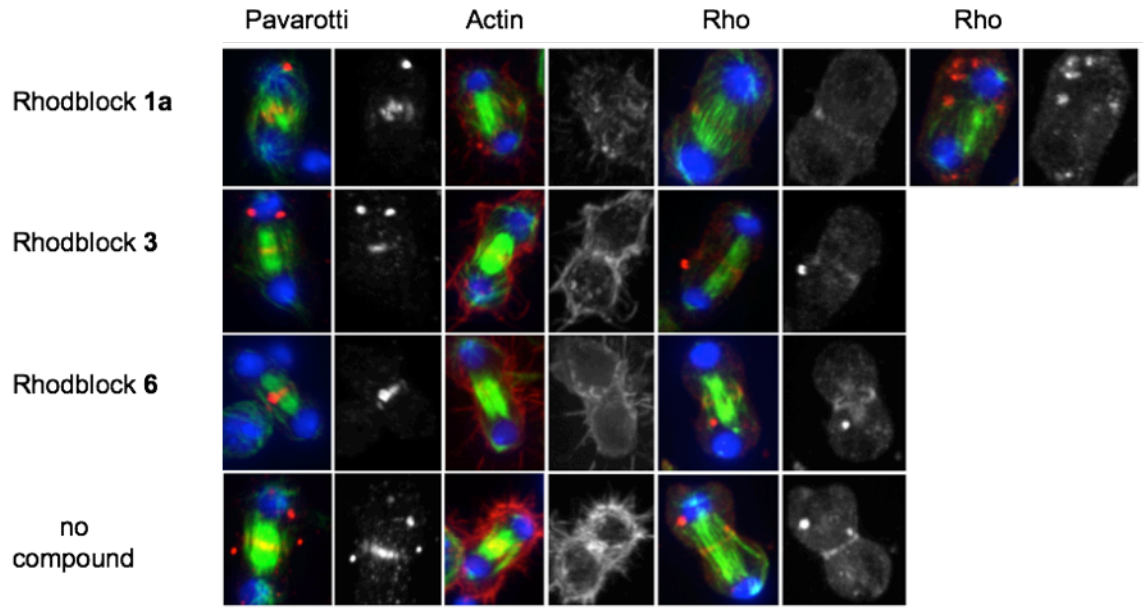

Supplementary Figure 9 *Effect of Rhodblocks on cytokinesis protein localization*. Pavarotti, Actin and Rho are shown in red in the color-combined figure and again for greater clarity in grey in the neighboring image. Microtubules are shown in green and DNA in blue. Note how Actin is missing from the furrow in Rhodblock **1a**-treated cells. Two images are shown for Rho staining in Rhodblock 1a-treated cells because Rho was mislocalized in some, but not all cells. Pavarotti localization is not perturbed by any Rhodblocks.

Nature Chemical Biology: doi: 10.1038/nchembio.363

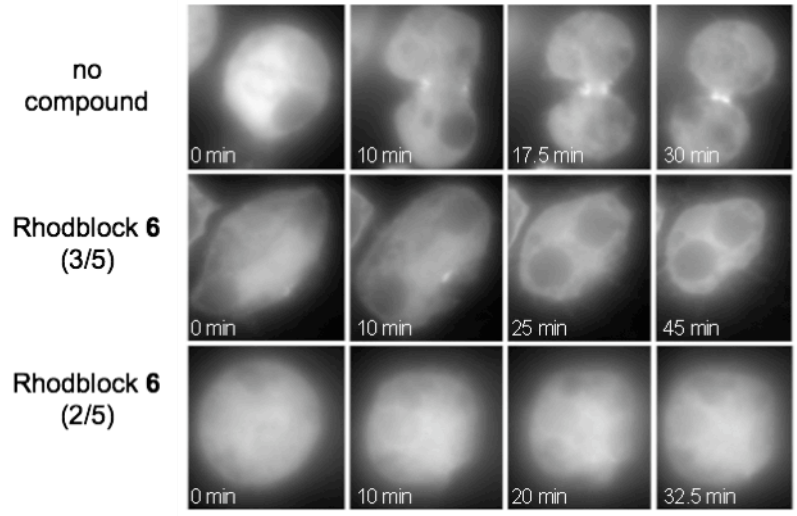

Supplementary Figure 10 *Movie stills of GFP-MRLC S2 cells treated with 200μM Rhodblock 6.* GFP-MRLC did not form a cleavage furrow in any of the 5 movies we took. In two movies (see bottom panel), cells failed to elongate and there was no ingression. In 3 movies (see middle panel) cells elongated, but did not ingress.

Nature Chemical Biology: doi: 10.1038/nchembio.363

Supplementary Table 1. Small molecule screening data

Category	Parameter	Description
Assay	Type of assay	Cell-based
	Target	Rho1 Pathway (Uniprot Accesion no. P48148)
	Primary measurement	Detection of Binucleate cells
	Key reagents	H33342 DNA stain (Sigma, B2261) and NHS-TMR Whole-cell stain (Invitrogen, C1171)
	Assay protocol	Detailed in *RNAi-sensitized small molecule screen* in Methods
	Additional comments	Precise timing of RNAi and dsRNA concentration should be optimized for each batch of Kc_{167} cells and dsRNA preparation
Library	Library size	Approximately 38,000 total
	Library composition	Known bioactives, natural products and drug-like molecules
	Source	Known bioactives collection from Biomol, fungal extracts (ICBG 2 and 4), the Starr foundation library, ChemBridge3, ChemDiv5 and ChemDiv4 libraries
	Additional comments	Visit the ICCB-Longwood website for library details (http://iccb.med.harvard.edu/screening/compound_libraries/index.htm)
Screen	Format	384-well
	Concentration(s) tested	100nl of 5mg/ml (compound) or 15mg/ml (natural product) in DMSO was pin transferred into 40□l cells and media
	Plate controls	Screening plates included wells containing Rho RNAi alone-treated cells
	Reagent/ compound dispensing system	Seiko and Epson compound transfer robots (http://iccb.med.harvard.edu/screening/technology_screen_facil/compound_transfer_robot.htm)
	Detection instrument and software	Molecular Devices ImageXpress Micro and MetaXpress software http://iccb.med.harvard.edu/screening/technology_screen_by_imag/info_Imagexpressmicro.htm
	Assay validation/QC	Assay was validated by screening the known bioactives collection from Biomol. Please refer to Supplementary Table 2 for details.
	Correction factors	N/A
	Normalization	N/A
	Additional comments	Screening was performed at the ICCB-Longwood (http://iccb.med.harvard.edu/)
Post-HTS analysis	Hit criteria	The mean percentage binucleate cells was calculated for wells treated with Rho RNAi alone. Enhancers were then scored as potential hits if they had a Z score greater than 2. Hits were then confirmed by visual inspection.
	Hit rate	0.03% (9 enhancers were identified while screening 35,486 drug-like compounds from the ChemDiv4, ChemDiv5 and ChemBridge3 libraries). Natural products and known Bioactives are not included in this calculation.
	Additional assay(s)	Initial hits were retested in the original assay
	Confirmation of hit purity and structure	Compounds were repurchased (ChemDiv and ChemBridge) and purity was verfied analytically
	Additional comments	N/A

Nature Chemical Biology: doi: 10.1038/nchembio.363

Enhancers and Suppressors			
Compound	**Total Object Count**	**Positive Object Count**	**% Binucleates**
latrunculin B	595	330	55
tunicamycin	535	268	50
W7	497	213	43
trifluoperazine	453	192	42
ML7	564	230	41
brefeldin A	654	271	41
paxilline	651	257	40
H7	737	296	40
cytochalasin D	333	131	39
cytochalasin B	314	124	39
Rho RNAi alone	492	122	25
doxorubicin	128	1	1
actinomycin D	277	23	8
puromycin	96	10	10
2-methoxyantimycin A	196	21	11
LY-83583	170	21	12
5-iodotubercidin	295	42	14
ICRF-193	364	57	16

Supplementary Table 2. *Enhancers and suppressors from screen of known bioactives.* We screened the Biomol collection of known bioactives, (stock solutions in DMSO at ~10 mM and 1 mM, http://iccb.med.harvard.edu/screening/compound_libraries/bioactives_biomol2.htm). CellProfiler Analyst automated analysis data is shown. Enhancers are shown in red and suppressors in green. For each enhancer and suppressor, the total object count (total cells) and positive object count (binucleate cells) are derived from images taken at 2 distinct sites in a screening plate well. Hits were verified by visual inspection of images. For the Rho RNAi alone control, data is averaged from 30 wells (2 sites/well) present on screening plates. Note the low cell count for many suppressor compounds. These suppressor compounds are toxic and inhibit stages of the cell cycle prior to cytokinesis.

Nature Chemical Biology: doi: 10.1038/nchembio.363

Treatment	1a (10 mM)	1b (30 mM)	2 (30 mM)	3 (100 mM)	4 (30 mM)	5 (100 mM)	6 (100 mM)	7 (30 mM)	8 (30 mM)
SM alone	0.7%	1.3%	1.1%	0.5%	7.0%	0.4%	0.9%	0.4%	0.9%
Rho RNAi	2.6%	2.6%	2.6%	2.6%	2.6%	2.6%	2.6%	2.6%	2.6%
SM+Rho RNAi	48.8%	31.2%	14.7%	28.0%	27.3%	17.6%	12.3%	8.8%	13.7%
Synergy Ratio	14.7	8.1	4.0	9.0	2.9	5.9	3.5	3.0	4.0
Pbl RNAi	8.6%	8.6%	8.6%	8.6%	8.6%	8.6%	8.6%	8.6%	8.6%
SM+Pbl RNAi	20.8%	8.9%	38.8%	16.5%	31.6%	15.9%	24.0%	11.9%	18.6%
Synergy Ratio	2.3	0.9	4.2	1.9	2.1	1.8	2.6	1.4	2.0
RacGAP RNAi	0.1%	0.1%	0.1%	0.1%	0.1%	0.1%	0.1%	0.1%	0.1%
SM+RacGAP RNAi	1.7%	1.6%	1.3%	0.2%	11.9%	0.3%	0.7%	0.7%	1.1%
Synergy Ratio	2.1	1.1	1.1	0.4	1.7	0.7	0.6	1.5	1.1
Dia RNAi	1.3%	1.3%	1.3%	1.3%	1.3%	1.3%	1.3%	1.3%	1.3%
SM+Dia RNAi	2.7%	1.9%	6.5%	2.5%	19.1%	1.9%	2.9%	2.0%	1.8%
Synergy Ratio	1.3	0.8	2.7	1.4	2.3	1.1	1.3	1.2	0.8
CK RNAi	16.6%	16.6%	16.6%	16.6%	16.6%	16.6%	16.6%	16.6%	16.6%
SM+CK RNAi	12.8%	2.9%	12.6%	13.2%	18.8%	11.9%	13.4%	13.8%	13.0%
Synergy Ratio	0.7	0.2	0.7	0.8	0.8	0.7	0.8	0.8	0.7
ROK RNAi	0.2%	0.2%	0.2%	0.2%	0.2%	0.2%	0.2%	0.2%	0.2%
SM+ROK RNAi	0.9%	1.1%	2.2%	0.5%	10.7%	0.5%	2.2%	0.3%	1.3%
Synergy Ratio	0.9	0.7	1.7	0.7	1.5	0.8	1.9	0.5	1.2

Supplementary Table 3. *Corrected % binucleate cells (i.e. minus the background of 0.3%) and synergy ratios for Rhodblocks 1-8.* % binucleate was calculated from ~ 2000 cells in 2 sites/well. 2 independent experiments were conducted with similar results. The maximum possible synergy ratio depends on the level of individual action. To allow a large range of synergy ratios, we set the experimental conditions reflected in Table S1 such that the individual actions were small.

Nature Chemical Biology: doi: 10.1038/nchembio.363

Treatment	GSK269962A (1μM)	CT04 (0.5μg/ml)	Lovastatin (10 μM)
Inhibitor alone	6.1%	14.1%	2.1%
Rho RNAi	7.0%	7.0%	7.0%
Inh+Rho RNAi	29.3%	28.4%	8.9%
Synergy Ratio	2.3	1.4	1.0
Pbl RNAi	25.4%	25.4%	25.4%
Inh+Pbl RNAi	48.4%	39.9%	49.8%
Synergy Ratio	1.6	1.1	1.8
RacGAP RNAi	17.1%	17.1%	17.1%
Inh+RacGAP RNAi	40.5%	34.3%	32.6%
Synergy Ratio	1.8	1.2	1.7
Dia RNAi	1.0%	1.0%	1.0%
Inh+Dia RNAi	12.9%	24.0%	12.9%
Synergy Ratio	1.8	1.6	4.2
CK RNAi	20.4%	20.4%	20.4%
Inh+CK RNAi	20.9%	30.5%	18.5%
Synergy Ratio	0.8	1.0	0.8
Rok RNAi	1.0%	1.0%	1.0%
Inh+Rok RNAi	14.5%	23.5%	4.7%
Synergy Ratio	2.1	1.6	1.5

Supplementary Table 4. *Corrected % binucleate cells and synergy ratios for control treatments.* % binucleate was calculated from ~ 2000 cells in 2 sites/well. 2 independent experiments were conducted with similar results. The Rho RNAi background in this experiment is a little higher than in Table S1, making the absolute synergy ratios lower. It is evident, however, that these three treatments, which have different mechanisms of inhibitions, have different synergy ratio profiles.

Nature Chemical Biology: doi: 10.1038/nchembio.363

Treatment	6 (100μM)	1a (10μM)
SM	2.1%	2.2%
Rho RNAi	4.8%	4.8%
SM + Rho RNAi	14.2%	17.8%
SM + MBS RNAi	1.3%	2.8%
Rho RNAi + MBS RNAi	4.5%	4.5%
SM + Rho RNAi + MBS RNAi	8.7%	19.1%

Supplementary Table 5. *% binucleate cells for cells treated with myosin phosphatase RNAi in addition to Rho RNAi and Rhodblocks 1a and 6.* % binucleate was calculated from ~ 2000 cells in 2 sites/well. 2 independent experiments were conducted with similar results. Cells were treated with 4 μg/ml myosin phosphatase dsRNA for 5 days total. 3 days into the myosin phosphatase RNAi, cells received a 1 day Rho RNAi treatment followed by a 24h small molecule treatment as discussed in the Methods section. Note the decrease in the level of binucleate cells in MBS RNAi-treated cells treated with Rhodblock **6**, but not **1a**.

Nature Chemical Biology: doi: 10.1038/nchembio.363

Supplementary Table 6. *LCMS traces of Rhodblocks 1-8*
The samples were run on a multicomponent Waters HPLC/MS, with a 25%-100% water/methanol gradient over for 5 min

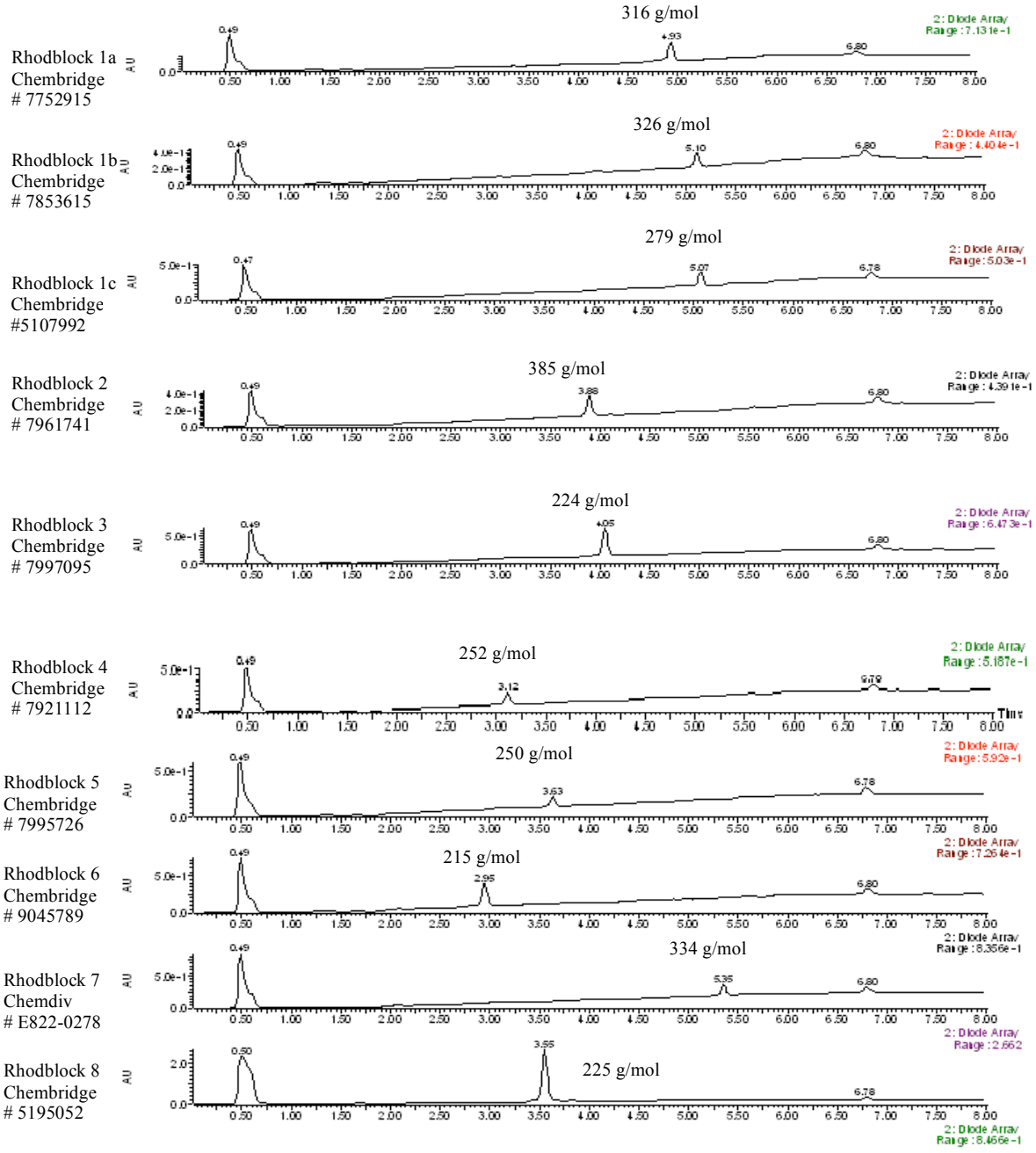

Nature Chemical Biology: doi: 10.1038/nchembio.363